Scientific Reports

https://doi.org/10.1038/s41598-026-43131-5

Article in Press

Patterned magnetic pole configurations in bonded magnets

Received: 29 September 2024

Accepted: 2 March 2026

Published online: 11 March 2026

Cite this article as: Behera M.P., Lv Y. & Singamneni S. Patterned magnetic pole configurations in bonded magnets. *Sci Rep* (2026). https://doi.org/10.1038/s41598-026-43131-5

Malaya Prasad Behera, Yifan Lv & Sarat Singamneni

Patterned magnetic pole configurations in bonded magnets

Malaya Prasad Behera, Yifan Lv, and Sarat Singamneni

Additive Manufacturing Research Centre

Auckland University of Technology Auckland New Zealand

Corresponding author: ***sarat.singamneni@aut.ac.nz***

Abstract

Additive manufacturing of bonded magnets using polymer extrusion, powder bed fusion, and stereolithography is established, but this paper focuses on the laser powder bed method. Magnetic particles mixed with polymer powders were consolidated into bonded magnets by selective laser sintering. External magnetic fields were applied to align particles during sintering, but with uniform powder compositions and fields, the effects of which were limited to bulk properties. Considering the point-wise material consolidation mechanics, we hypothesise that controlled dispersion of multiple powder materials and localised external magnetic fields in specific orientations and at specific times during sintering can lead to bonded magnets with controlled magnetic heterogeneity. Results from experimental research conducted and reported in this paper have shown this hypothesis to be true. The outcome of this research paves ways towards achieving bonded magnets with controlled placement of different magnetic materials. The as-printed samples exhibit relatively weak polarisation (≈1.5–2 mT flux), but magnetisation under external fields (1.5–1.9 T) raises flux values up to 6 mT N / 3 mT S for NdFeB/FeSi and 14 mT N / 6 mT S for NdFeB/FeCo, demonstrating strong amplification of polar strengths. Both NdFeB/FeSi and NdFeB/FeCo samples show 80–100 mT North and 50–100 mT South differential polarities under external fields, with minimal change from as-printed to magnetised states. Even when the external field is reversed, a persistent North-upward remanent tendency confirms an easy-axis alignment induced during laser consolidation.

Key words: laser sintering, bonded magnets, multi-materials, multi-polar, controlled magnetism

Introduction

The much-adored design freedom over traditional methods and the rapid technological growth with wider materials options advanced the additive manufacturing methods towards ever increasing applications. Manufacturing of complex shaped magnets based on both hard and soft magnetic material options is one of the intriguing developments in the recent past. From the basic fused filament to the more advanced laser sintering and melting techniques, there have been many attempts to process different magnetic materials by the additive technologies. The current research is mainly focussed on the additive manufacturing of bonded magnets, which involves the consolidation of magnetic particles within polymer substrates based on one of the polymer printing technologies. Fused deposition modelling (FDM), stereolithography (SLA), and selective laser sintering (SLS) are the common methods used, while there is also some progress towards the use of external magnetic fields in all these cases.

Polyamide polymer filaments loaded with rare earth NdFeB magnetic powders were evaluated for additive fabrication of bonded magnets by FDM [1 and 2]. The magnetic characteristics of the printed samples vary with the content of the magnetic filler material by weight, but excessive loading will

embrittle the filaments and affect the thixotropic attributes essential for the coalescence of fused filaments. Within these limits, magnetic remanence and coercivity values 310 mT and 740 kA/m [1] and 580 mT and 708.2 kA/m [2] respectively have been reported. Considering the easy access and lower costs FDM has been a common additive processing option for low end applications, but the quality and consolidation issues often limit the wider use in more serious engineering applications.

Polymer composite slurries with nano iron oxide particles suspended in a UV curing resin consolidated by SLA were analysed for the magnetic characteristics observing randomly oriented magnetic domains resulting from the uncontrolled dispersion and orientations of the nano magnetic particles within the UV cured polymer substrates [3]. The magnetic anisotropy effects were reported to cause a dipolar coupled system, where the magnetic domain interactions might demagnetise the material. A comparative assessment of the magnetic property responses of bonded NdFeB magnets produced by FDM, SLS and SLA revealed better magnetic remanence and coercivity responses based on the UV cured magnetic components [4].

Bonded magnets were produced and analysed using the laser powder bed process SLS, based on mixed feedstock of spherical NdFeB and polymeric binder polyamide powders [5]. Parametric studies considering laser power, scan speed, binder content, layer thickness, and hatch spacing and

mechanical and magnetic responses revealed magnetic remanence 330 mT, intrinsic coercivity 696 kA/m, and maximum energy product 17.1 kJ.m^3 with a binder content of 6% and lower laser energy density and layer thickness values. Mapley et al [6] explored SLS of bonded NdFeB permanent magnets from mechanically mixed isotropic powders with flake and spherical morphologies. It was found that magnets produced from spherical powders demonstrated superior density and magnetic properties compared to those from flaky powders, with residual induction values of 362 mT and 302 mT, respectively. The magnetic performance was lower compared to the industry-standard injection moulded magnets, primarily due to lower powder loading fractions, indicating the need for the use of anisotropic powders and in-situ alignment fixtures to further enhance the process attributes. The effects of the loading fractions of NdFeB powders in spherical and flaky forms on the mechanical and magnetic responses after laser sintering into permanent magnets bonded in Nylon were evaluated relating the application specific compositions [7].

With the 3D to 4D printing evolution, consolidation of magnetic powders in soft polymeric substrates by all three common processing routes, FDM, SLA, and SLS attracted some attention recently, considering the convenience in achieving the post-printing shape-shifting attributes under external magnetic fields. Polymer composite filaments of PLA loaded with varying mass fractions of Fe_3O_4 were used to fabricate complex structures by FDM. The shape memory responses of the printed structures were reported to be

significant under external magnetic field stimulations [8]. Magnetic gripper structures fabricated by selective laser sintering of $Nd_2Fe_{14}B$ plus thermoplastic polyurethane polymer composite powders with varying weight ratios were evaluated for the shape shifting responses under external magnetic fields. The magnetic force was reported to be closely related to the content and the inter-particle distances of the magnetic filler particles in the printed substrates [9]. Also, polymer filaments based on PLA, thermoplastic polyurethane and NdFeB blends were processed by FDM and the resulting structures were shown to exhibit good shape memory responses under thermal and thermo-magnetic stimuli [10].

Energy coupled manufacturing refers to the use of electrical or electromagnetic fields applied during manufacturing to achieve specific structural or mechanical properties. External magnetic fields are also used to algin the magnetic responses of a product in preferred directions. The possibility of producing bonded magnets using the additive technology as discussed above also attained some attention towards energy coupled additive manufacturing to control the magnetic behaviour of the printed parts. Polymer composite filaments made of iron particles filled in PLA were processed by field assisted FDM demonstrating enhanced and anisotropic susceptibilities [11]. Sarkar et al presented a Multiphysics model to simulate the magneto-viscous mechanisms in substrates printed by FDM of polymer filaments loaded with magnetic powder particles under external magnetic field applied parallel to the build plate [12]. The model predicts

that the degree of alignment of the magnetic particles in the printed substrate will vary with the filler fraction, field strength, and the print speed. The magnetophoretic force was found to be less significant compared to the drag forces on the particle during the sintering stages of the polymer matrix. External magnetic fields applied by placing permanent magnets on either side of the printed substrates in a FDM system based on polymer filaments loaded with magnetic particles demonstrated permanent deformations in the direction of the theoretical magnetic force lines due to extrinsic strains [13].

Mapley et al. explored the enhancement of magnetic properties in bonded permanent magnets fabricated using SLS under a 20.4 mT magnetic field applied by a Helmholtz coil to align anisotropic neodymium-iron-boron (NdFeB) particles during the consolidation of the polymer composite powders [14]. The experimental results demonstrated the alignment field introducing significant anisotropy in the bonded magnets and improved crystal orientation. The viscous drag forces are quite dominating as against the magnetophoretic forces in both FDM and SLS as the fused filaments and softened polymer pools are sintered and solidified quickly. Relatively, there is a better opportunity to align the magnetic particles along the magnetic force lines of external fields in SLA [15-19].

Kokkinis et al demonstrated a multi-material magnetically assisted direct ink writing process to achieve controlled particle orientation by means of

an external magnetic field applied during the UV curing stage [15]. The inks used are UV curing polymer resin composites with preloaded magnetic particles or platelets and the printed parts with controlled magnetic particle orientations can change shapes in response to specific external stimuli. Maghemite-Multiwalled carbon nanotubes loaded into an acrylic resin and then 3D printed by UV curing the liquid polymer composite under external magnetic fields demonstrated superior magnetic properties and directional alignments of the filler particles [16]. An external field assisted mask image projection stereolithography system was used to consolidate acrylic polymer blends with magnetic particles [17]. The external magnetic field assisted in moving the magnetic particles to desired locations. Direct ink writing of elastomer composites loaded with magnetic ferromagnetic particles under the influence of external magnetic fields to control the orientation of the magnetic particles was reported demonstrating patterned magnetic polarity in the filaments printed [18]. Programmed ferromagnetic domains were achieved in 3D forms leading to remotely controlled auxetic forms and shape-shifting attributes. Photosensitive resin blends with strontium ferrite particles processed by polymer jetting method led to controlled particle alignment with the use of external magnetic field generated by a couple of NdFeB permanent magnets placed on either side of the printed substrate [19].

Zheng, J. et al. proposed and evaluated a novel high-temperature superconducting (HTS) pinning maglev concept that integrates propulsion

via a double-sided homopolar linear synchronous motor (H-LSM), aiming to achieve an economical self-stabilizing high-speed system with strong propulsion–levitation–guidance (PLG) capability. Analytical and numerical simulations and benchmarking against the conventional permanent-magnet LSM (PM-LSM) proved the 19-ton prototype to be competitive in terms of performance and cost. To capture system-level feasibility, they further introduced a lateral dynamic response (electro-mechanical coupling) analysis to assess how propulsion interacts with levitation dynamics during operation. Overall, their results indicate the proposed HTS pinning maglev with H-LSM can satisfy propulsion requirements while maintaining favourable macroscopic dynamic behaviour for high-speed running, with the H-LSM offering a lower-cost pathway compared with PM-LSM designs [20].

Evidently, the application of the common additive manufacturing methods to fabricate bonded magnets with different material combinations is established. Energy coupled AM approaches integrated into the additive consolidation of bonded magnets with controlled magnetic particles dispersions is also known. However, the dispersion of the magnetic particles and the controlled consolidation by the external fields have so far been confined to the bulk, targeting uniform dispersions and properties all around the printed substrates. Also, the magnetic field induced extrinsic strains proposed to be a way to control the geometrical shapes of the printed objects with magnetic particle blended polymer slurries does not

appear be a real promising opportunity. With the unlimited freedom which is an inherent trait of polymer additive manufacturing to achieve any complex shapes, using external magnetic fields to alter shapes during printing is not meaningful. The current research takes the opportunity to the next level, fully exploiting the point-by-point consolidation of the laser powder bed fusion SLS process to achieve controlled variation of both the candidate materials as well as the post-process magnetic responses of the printed substrates. Custom methods developed for controlled powder dispersion and external magnetic fields applied from below the print bed are integrated into a makeshift SLS system to demonstrate controlled magnetic heterogeneity in the printed substrates.

The novelty of this research lies in addressing two specific gaps: (i) the consolidation of magnetic and polymer blends by laser sintering under controlled external fields, and (ii) the realisation of multi-material consolidation involving hard, soft, and non-magnetic material combinations by selective laser sintering. This innovation is further reflected in overcoming the technical challenges of achieving both precise magnetic field control within the laser sintering chamber and controlled dispersion of multiple materials across the powder bed. Both challenges have been addressed through innovative solutions that are currently at the provisional patent stage. Controlled magnetic heterogeneity has long been sought in electromagnetic designs, yet it has received limited attention due to manufacturing constraints. Previous attempts have typically relied on

assembling conventionally produced magnets into fixtures designed to achieve variations in magnetic orientation across a component. In contrast, the possibility of creating Halbach arrays with inherently controlled magnetic arrangements, as well as realising functionally graded magnetic properties, offers highly attractive prospects for modern electromagnetic device design. The present research establishes proof-of-concept for a technology capable of delivering these advances, paving the way to explore key new scientific challenges such as:

- How energy coupling to manufacturing, based on electromagnetic fields, enables control of magnetic heterogeneity in bonded magnets
- The possibilities of achieving complex yet controlled interactions in the magnetic fields within substrates made of multiple magnetic material combinations

Materials and methods

Experimental design and mechanisms

A make-shift selective laser sintering system developed inhouse at AUT based on a 60 W CO_2 laser as shown in Fig 1 (a) is used for all the laser sintering experimental trials. Considering the high absorptivity of both materials investigated, the specimens were sintered using a CO_2 laser (Firestar vi30, Synrad Inc.) operating at a wavelength of 10.6 µm and emitting a Gaussian beam. The experimental process parameters included a laser power 18 W, a laser scanning speed of 500–1000 mm s^{-1}, a

characteristic laser spot radius of 0.27 mm, and a layer thickness between 0.10 and 0.20 mm. Fig 1(b) is a schematic showing the arrangement of the external electromagnets assembled under the build platform which is one of the several such embodiments included and claimed in a non-provisional patent application filed by the authors. As depicted in Fig 1 (c), the wiper blade design is altered replacing by a guided bar which supports a number of small hopper devices. These hoppers can be moved along the guide rails on the bar and positioned either to extract or deposit powder particles at different locations on the powder bed as needed by the controlled magnetic part design. One of the hopper devices is connected to a suction system for removing the base material powder from the bed selectively and as per the part design. The other hoppers hold different magnetic powder materials and can be moved to different locations on the powder bed combining the motion of the wiper blade together with their own translational motions along the axis of the wiper blade.

A controlled opening mechanism at the orifice of each of the powder dispensing hoppers as detailed in Fig 1 (d) allows the dispensing of controlled quantities of different magnetic powders at specific locations on the powder bed as per the part design specifications. With the localized removal of base matrix material and refilling with different magnetic powders within those locations will allow to produce multi-material magnetic substrates with the properties ranging from non-magnetic to magnetic or soft magnetic to hard magnetic combinations with the polar directions of specific locations varied as needed. The following is the normal

sequence of operations to achieve multi-material magnetic consolidation using these specially designed systems:

- The base polymer material is spread in the usual manner as on any commercial system using the normal working mechanism of the wiper blade.
- The additional powder dispensing mechanisms mounted on the wiper blade come into action next. Coordinating the movement of the wiper blade and the relative positioning of the hopper heads on the cross rails to move different nozzles to the required locations.
- The powder suction nozzle is first moved to the specific locations and operating the vacuum suction mechanism, the required quantity of the base powder from that layer is removed.
- Then the respective powder dispensing bins are brought to specific locations and the miniature powder dispenser mechanism is operated to drop calculated quantities of different magnetic powders into these depleted areas one after the other.
- Once this step is completed, the laser sintering is applied to consolidate these base powders together with the magnetic powders to achieve the multi-material magnetic layers with controlled dispersion of magnetic and nonmagnetic materials and with hard and soft magnetic materials dispersed as needed within the substrate.
- Just before, during, and/or just after the sintering and processes, the magnetic field based on the electromagnetic assemblies under the build platform are operated to additionally control the magnetic

orientations of the islands of magnetic materials consolidated as preferred.

- The consolidation of different materials in different regions is achieved with carefully controlled process conditions as per the material processing mechanics.

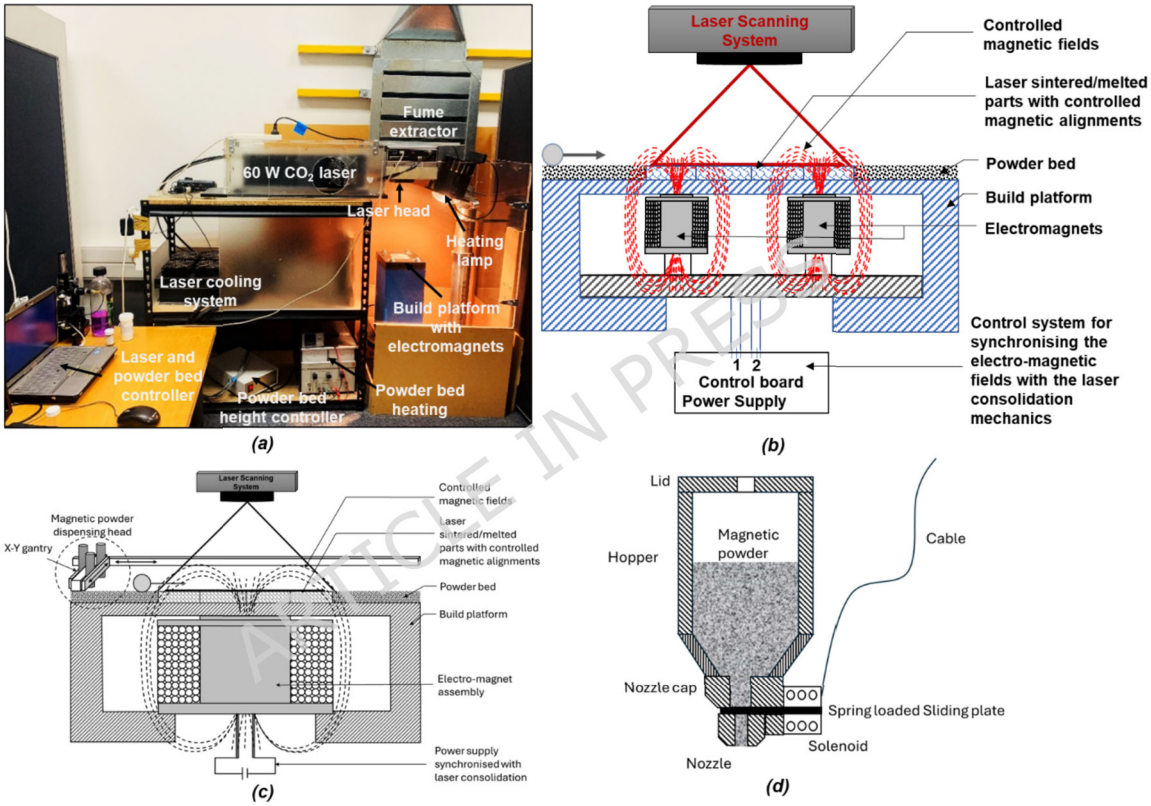

Fig. 1 Laser sintering experimental setup (a) the make-shift laser sintering system based on a 60W CO_2 laser, (b) the schematic arrangement of external magnetic fields under the build plate following one of the embodiments in the non-provisional patent application filed by the authors, (c) a detailed rendering of the

selective suction and powder dispensing arrangements, and (d) a schematic of the selective powder dispensing hopper mechanism

Test specimens, materials, and magnetic characterisation

The schematic representation of the samples built with a dual electromagnetic layout under the build plate is depicted in Fig 2 (a). While the experimental system developed allows to use multiple magnets under the print bed as needed, in this initial work, only two magnetic islands are created in all the samples as in Fig 2(a), for the ease of understanding the compounding influences of complex magnetic fields from multiple sources. The electromagnets used have 32 axial and 6 radial winding configurations, giving a 230 mT external field applied to the laser powder consolidation zone. The direction of the fields applied by these two magnets can be changed by changing the direction of flow of current through the coils. The nylon matrix powder is first spread on the powder bed and then a custom-made powder dispensing system as per a design currently submitted as another provisional patent by the authors is employed for the deposition of controlled quantities of different magnetic powders in each layer. Once the magnetic powder is in place, a thin layer of nylon is also added on top before laser sintering and consolidating the layer. A set of grid points as shown in Fig 2 (b) are used to make the magnetic field measurements using the Gauss probe method. The specimens produced have dual magnetic islands embedded into the

polymer matrix, with either NdFeB and FeSi or the NdFeB and FeCo combinations as depicted in Fig 2 (c) and (d) respectively. The samples are built with a total of 5 layers of 50µm thickness each.

The controlled spatial organisation of magnetic particles within the polymer matrix is expected to result in patterned magnetic pole configurations as also evaluated earlier by Zhou et al [22]. The polymer content and processing conditions can be exploited to achieve controlled engineering of the binder and particle interactions and the resulting magnetic particle distribution patterns. This is an immediate opportunity in controlling the magnetic landscapes of bonded magnets effectively utilising the inherent characteristics of the layer-wise consolidation of polymer blends by laser sintering, The use of external magnetic fields adds a new dimension of control over such controlled magnetic patterns. Apart from the binder flow conditions and hydrodynamic forces during sintering, the external magnetic field applies field forces to further align the magnetic particles in preferred directions. This allows controlling not only the dispersion patterns of the magnetic particles within the polymer matrix but also preferred orientations of the polar regions within the consolidated matrix.

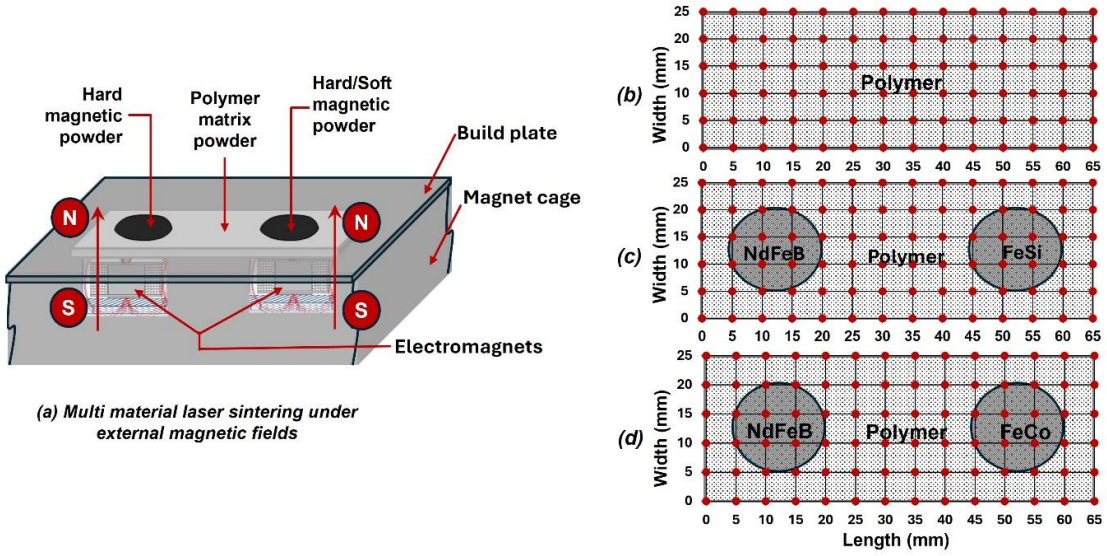

Fig. 2 Schematic of the laser sintering setup (a) Dual magnetic layout for energy coupled laser sintering (b) grid points for magnetic field measurements on the printed samples (c) controlled magnetic NdFeB and FeSi islands in nylon matrix, and (d) NdFeB and FeCo islands in nylon matrix.

A high voltage capacitive magnetiser, Model DXMM-20C70 is used for magnetising the printed samples. The thin printed samples of five layers, with the magnetic particles embedded and aligned as needed are carefully inserted on to a fixture which is then loaded on to the magnetiser, assuring the directionality of the applied field as per the orientation of the sample. The magnetic field strengths at pre-set points on the printed specimens as shown in Fig 2 (b) to (d) are measured before and after magnetisation using a Gauss meter, Model DX-102, made by Dexing Magnet Ltd., China. SEM images of the powder particles of the base matrix nylon, hard magnetic NdFeB, and soft magnetic FeSi and FeCo are shown in Fig 3 (a), (b), (c), and

(d) respectively. EDS analysis results indicate the compositions of the three magnetic materials to be:

- ***NdFeB:*** Nd 11.7%, Fe 77.16%, B 8.51%, P 1.11%, Al 0.15%, Cu0.28%, Pr 0.83%, and Si 0.27% by weight
- ***FeSi:*** Fe 96.5% and Si 3.5% by weight
- ***Fe35Co:*** Fe 64.33% and Co 35.38% by weight

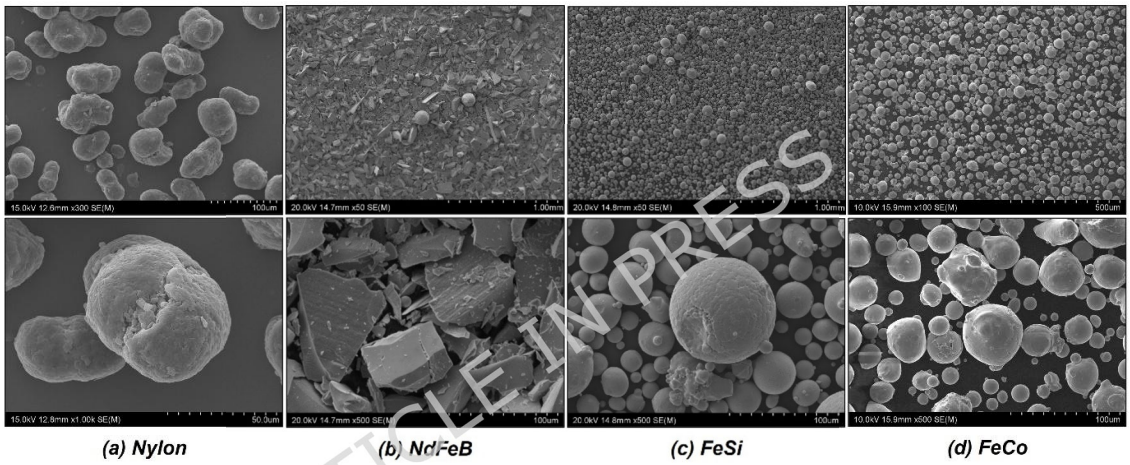

Fig. 3 SEM images of the powder feedstock of (a) Nylon, (b) NdFeB, (c) FeSi and (d) FeCo

Results and discussion

External field vs meso-structures

SEM images based on nylon plus FeSi composite powder samples laser sintered with and without the use of external magnetic fields are shown in Fig. 4 (a) and (b) respectively. A quick comparison clearly elucidates that the external magnetic field has an influence in ordering the consolidation

of the polymer composite into uniformly distributed clusters under the influence of the field lines (Fig 4 (a)). The alignment of the partly fused and solidified polymer composite particles in parallel lines as evident in Fig 4 (b) is the common feature of laser sintered substrates with laser scan lines following parallel pathways on the surface imaged. This result clearly indicates that the characteristic meso-structural growth, predominantly governed by the raster path schemes, can be homogenised and transformed into uniform spherical alignments through the application of external magnetic fields. Although the influence of these external fields on the material–process–structure relationships is not the primary focus of this work, it is pertinent to note that the magnetic responses of the printed samples will also be affected by structure–property interactions arising out of the use of the external field.

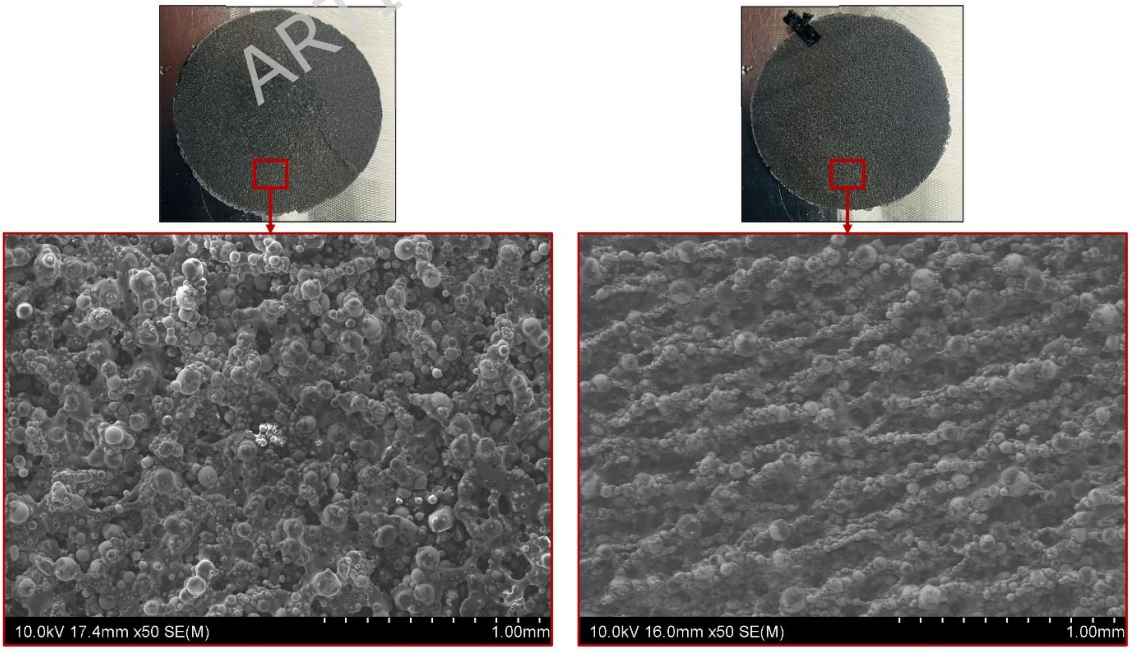

(a) Laser trails with magnetic field applied

(b) Laser trails with-out magnetic field applied

Fig 4 SEM images of nylon+FeSi composite powder samples laser sintered with 30 W power and 762 mm/s scan speed using parallel laser scan patterns (a) with and (b) without the use of external magnetic fields.

Controlled magnetic heterogeneity in as-printed state

To establish the role of the direction of the external applied field on the preferred orientation of the resulting magnetic poles in the printed part, the nature of consolidation of the magnetic powder embedded into the multi-material laser consolidation needs to be evaluated. For this, two samples are built with NdFeB particles used at both islands, but with the external field in the same and in opposing directions at the two magnets. The iso-magnetic fields plotted are shown along with the images of the printed samples and the directions of the external fields are shown in Fig. 5 (a) and (b) respectively. These samples are not magnetised yet and in the as-printed state they are already showing some remnant magnetism. The result of the dual magnetic fields acting simultaneously in the North upward direction has resulted in a north pole surrounding a central south pole at the two ends of the printed sample as seen in the contours on the top face of the sample in Fig 5 (a). However, the opposing field directions with the south upwards on the left and the north upwards on the right has given a predominantly south on the left and north on the right magnetic field distribution as evident in Fig 5(b). This is an initial proof of the hypothesis that controlled dispersion of magnetic particles in laser sintered substrates

with controlled external magnetic fields can result in controlled magnetic heterogeneity.

It is important to note that the dispersion of powder particles, followed by laser consolidation, may sometimes result in uneven consolidation of the magnetic particles. Furthermore, the application of an external magnetic field forces the redistribution of magnetic particles within the clusters formed in each layer. These factors collectively influence the final magnetic field responses at the polar regions. The scattered distribution of the field lines arises essentially from these underlying phenomena. More critically, when the top surface is constrained to have the same polarity as in Fig. 5(a), where both NdFeB islands are forced into a north-pole orientation, an in-plane splitting of the poles occurs. The close proximity of the same pole leads to opposing magnetic forces and consequently, the magnetic field segregates into two isolated south poles, surrounded by a split north pole, as evidenced by the iso-magnetic field contours presented in Fig. 5(a). At the same time, the option of a di-pole arrangement within a given plane of the printed sample facilitates the segregation of magnetic powder particles into a bi-polar configuration, with a predominant north and south pole, as shown in Fig. 5(b).

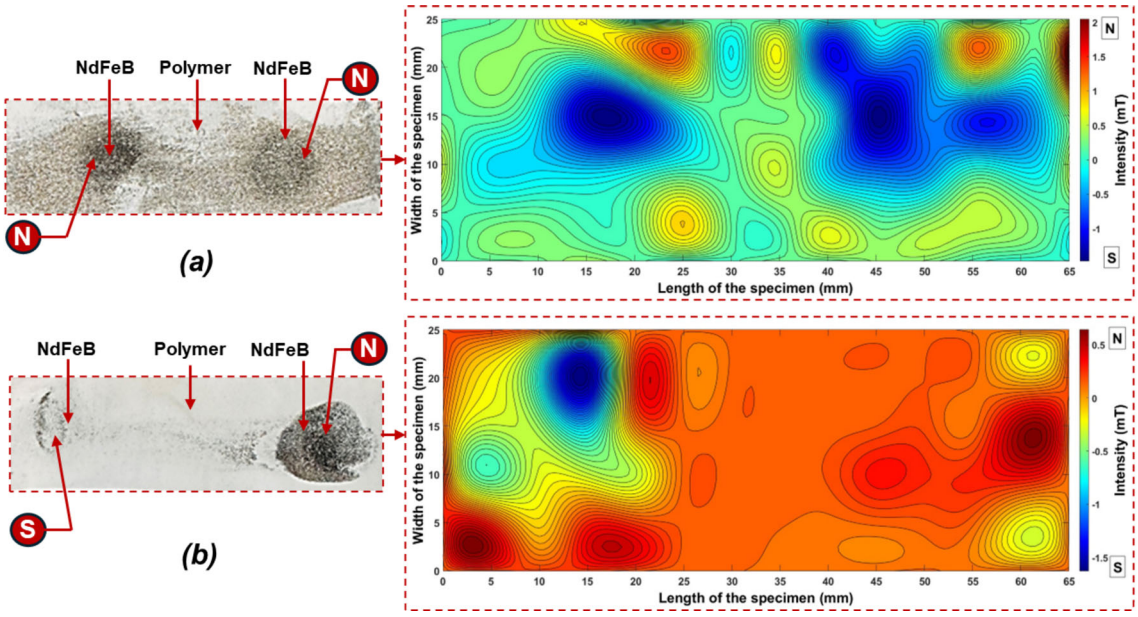

Fig. 5 Laser sintered samples with NdFeB islands created at both ends within nylon matrix and the iso-magnetic field contours plotted on the top surfaces with external magnetic fields (a) applied with north upward at both ends and (b) south upward on the left and north upward on the right

Post-printing magnetisation effects

The two printed samples are then magnetised under an external magnetic field at 1.5 T and the iso-magnetic field contours generated are presented in Fig. 6 (a) and (b) in the same order as for the samples in Fig 5 (a) and (b) respectively. For the sample produced with a north upward orientation at both ends, the north upward magnetic field applied has resulted in the splitting of the top surface with multiple localised dipoles as seen in Fig 6 (a). Evidently, this sample tends to achieve both north and south polar fields interspersed on the top surface due to the proximity of the two NdFeB islands with north upward magnetic easy axes imposed during

consolidation, as in the as-printed state (Fig 5(a)), while this effect is more pronounced after magnetising under the external field.

However, magnetisation under external field further consolidated the expected south to the left and north to the right configuration in the case presented in Fig. 6(b). However, there is a localised north-south split at the left end as the dominant northward pole on the right appears to have some influence in the magnetisation of the left end under the external field. The tendency of the North-south split at the left end is a common feature in this sample before and after magnetisation as obvious comparing the contours in Fig 5(b) and Fig 6(b), but with a more pronounced result in the latter case, under the influence of the magnetisation with the external field. Further, under a field of 3.5 T with the north upward direction, the sample with both NdFeB aligned with a north upward orientation magnetised as shown in Fig 6 (c). Comparing the results of Fig 5(a), Fig 6(a) and then Fig 6 (c), for the same sample, the tendency to split into multiple north and south pole regions converged into a predominantly north-pole region spread all around, with the two south poles strongly magnetising at 5 mT around the two NdFeB islands. While there are minor variations, which might have occurred due to variations in compositions and dispersion levels of the NdFeB during multilateral dispersion and selective laser sintering, the magnetic field contours are largely symmetrical in this case across the surface examined as in Fig 6 (c).

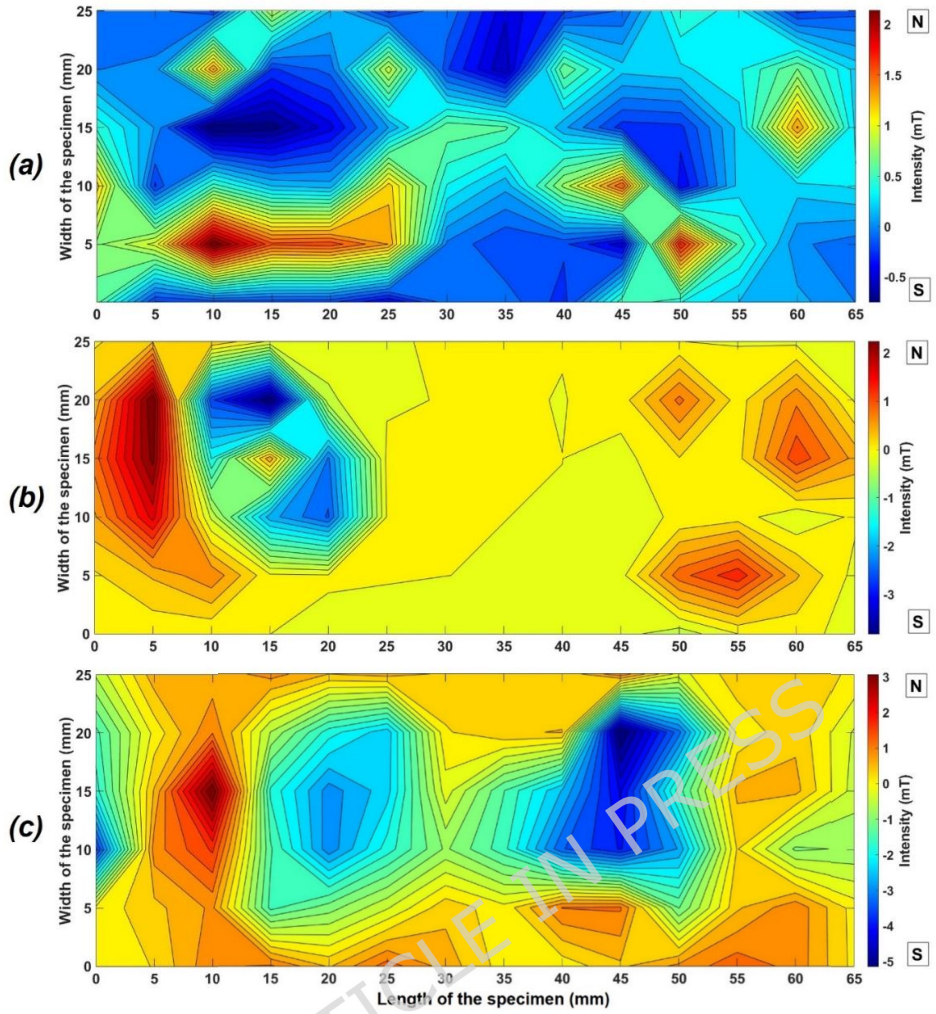

Fig. 6 Iso-magnetic field lines plotted on the top surfaces of samples (a) with both NdFeB islands printed with a north upward field and then magnetised with a north upward field of 1.5 T, (b) with NdFeB islands printed with a south upward field on the left and a north upward field on the right and then magnetised with a north upward field of 1.5 T and (c) the sample as in (a), after magnetising with a 3.5 T north upward field.

Multi-material magnetic substrates

To establish multi-material sintering under magnetic fields, specimens were fabricated using NdFeB/FeSi and NdFeB/FeCo combinations, with two

islands printed at either end of the bar samples. Laser sintered samples, bitter images obtained spreading ferrofluid on a thin glass plate kept over the specimen top surface and the iso-magnetic field lines obtained by Gauss-mater measurements on the top face are presented in Fig 7. The sample with NdFeB and FeSi islands is in Fig 7 (a) and that with the NdFeB and FeCo islands is in Fig 7 (b) while the polymer matrix is nylon in both cases. North upward external magnetic fields of 230 mT are applied under each island during sintering to achieve an upward magnetic easy axis on either side.

In the as-printed state, both samples showed a north magnetic field at the centre on the left side of around 2 mT, surrounded by a circular south pole that is split into many regions of varying intensities. The entire right region is showing no magnetic field as the soft magnetic island would have no remnant magnetism in the absence of any external field. The bitter images also confirm these results as there is an accumulation of the ferro fluid in a dark circular form on the left side, which is corresponding to the north central and south circular magnetic field orientation observed in the contour plots in the NdFeB hard magnetic regions. Apparently, the magnetic flux lines generated by the applied external magnetic field lead to a concentrated upward north orientation of the NdFeB particles at the centre, while a surrounding circular hollow region of south polarity forms around them. This effect is likely repeated in every layer. The ferrofluid is completely unaffected in the areas towards the right end in accordance with

the absence of any field in the soft magnetic FeSi and FeCo regions in Fig 7(a) and Fig 7 (b) respectively.

After magnetising in a north upward 1.9 T field, these two samples resulted in magnetic field distributions as shown in Fig 8, which are very similar to the ones in Fig. 7. The areas central to the NdFeB island on the left are predominantly north with a circular spread of the south pole all around, with varying field strengths. The maximum strength of the northward field strength is 6 mT in the first case as in Fig 8 (a), while the second case with NdFeB and FeCo islands reached a maximum of 14 mT. These variations are mainly due to the varying dispersions of the hard magnetic NdFeB particles using the make-shift powder dispensing and dispersion arrangements employed. It may also be noted that the regions to the right have shown no remnant magnetism due to the soft magnetic nature of the FeSi and FeCo phases present.

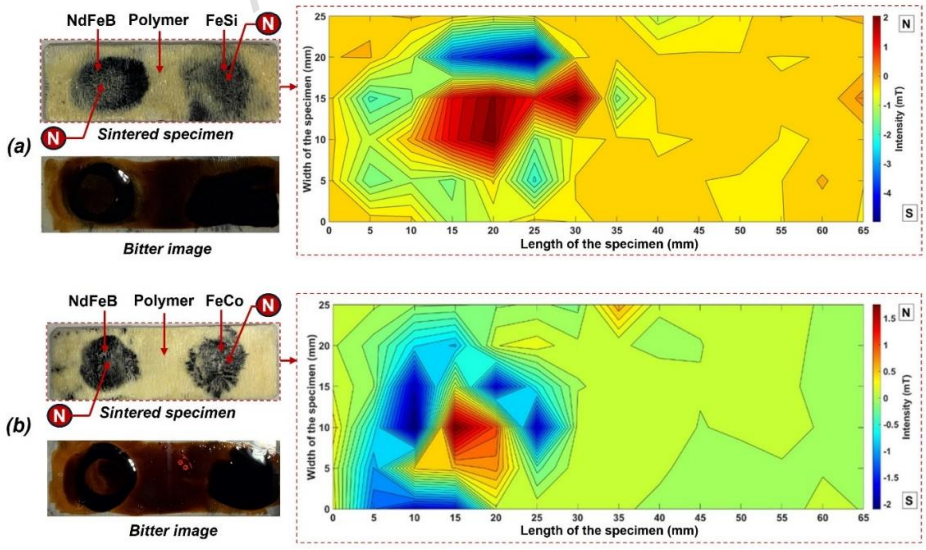

Fig. 7 Laser sintered multiple magnetic material samples in nylon matrix, bitter images, and Iso-magnetic field lines plotted on the top surfaces before magnetising with (a) NdFeB on the left and FeSi on the right and (b) NdFeB on the left and FeCo on the right

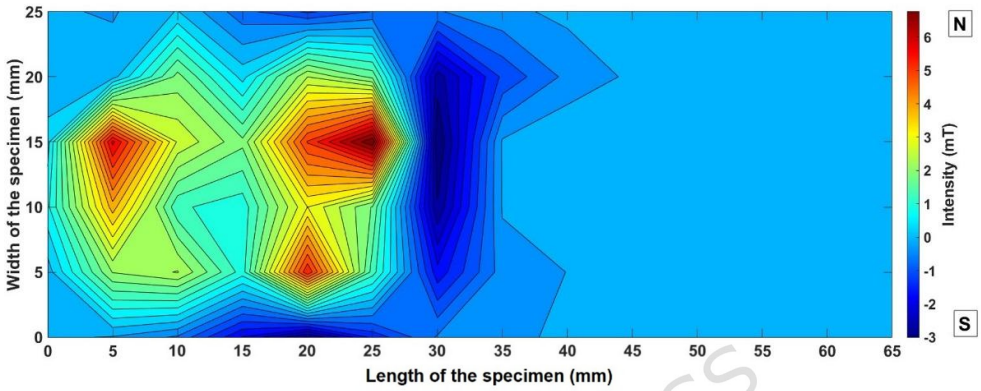

(a) NdFeB on the left and FeSi on the right

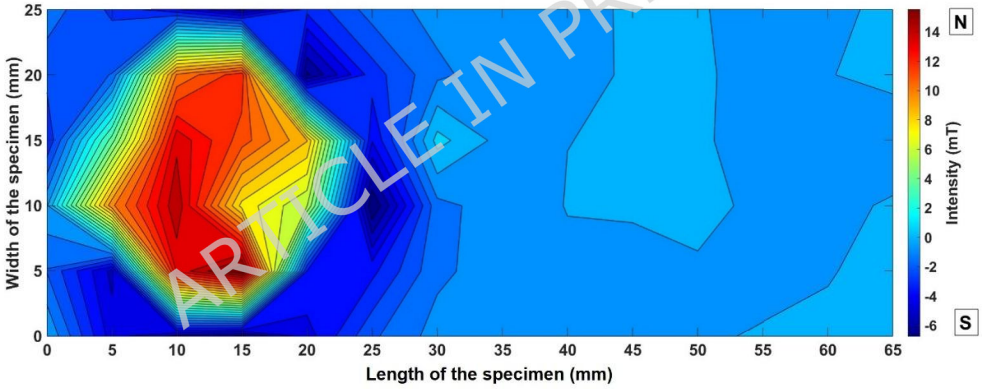

(b) NdFeB on the left and FeCo on the right

Fig. 8 Iso-magnetic field lines plotted on the top surfaces of laser sintered multiple magnetic material samples in nylon matrix after magnetising under a north upward 1.9 T field (a) with NdFeB on the left and FeSi on the right and (b) with NdFeB on the left and FeCo on the right

In order to establish the role of the soft magnetic regions in the overall scheme of the magnetic field variations, it is necessary to examine these

samples in an active external field. However, considering the relatively low magnetic permeabilities of these samples due to the small quantities of the magnetic materials present, any external field will have a dominant role and needs to be filtered out to capture the true role of the magnetic material dispersions within these sintered samples. This is resolved by using a simple differential calculation method. Two permanent magnets of 230 mT each are kept side by side and north upwards, at the same distances as the two magnetic islands in the sintered samples. A plain polymer plate of the same dimensions as the test pieces is sintered with pure nylon and is used first, to measure and plot the actual field line configurations generated by the two permanent magnets. This will then serve as the control in the measurement of the influence of the actual test specimens. The two test specimens are then placed one after the other on these permanent magnets for measuring the magnetic field values at the same points as the control. The difference between the control readings and those with the actual specimens are used as a measure of the role of the multi-material magnetic specimens. The differential magnetic field contours obtained thus in the case of the samples with NdFeB/FeSi and NdFeB/FeCo islands before applying any external magnetic field are presented in Fig 9 (a) and (b) respectively. These results clearly elucidate the north upward orientation of the field central to both magnetic material islands in both the samples. The south pole field lines are surrounding the two north pole regions with a staggered variation of intensities. While there is a general tendency for the central regions to achieve a south ward field, the NdFeb/FeSi sample showed a zero-field zone in between the two

magnetic material islands, which is typical of the polymer matrix present there as in Fig 9 (a). However, the NdFeB/FeCo case in Fig 9 (b) resulted in a widely spread south polar region between the two magnetic islands, possibly due to the relatively stronger north pole regions at 100 mT, that are focussed close to the central axes of the magnetic material axes.

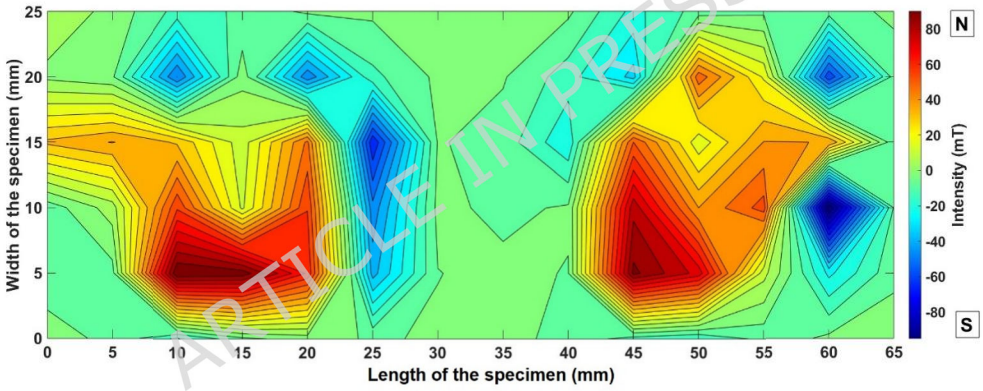

(a) NdFeB on the left and FeSi on the right

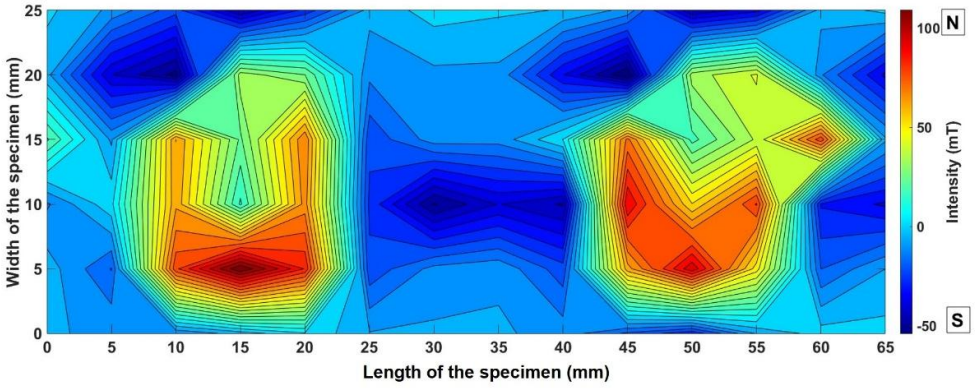

(b) NdFeB on the left and FeCo on the right

Fig. 9 Iso-magnetic field lines plotted on the top surfaces of laser sintered multiple magnetic material samples in nylon matrix before magnetising and with a north upward external magnetic field of 230 mT acting under the two islands (a) with NdFeB on the left and FeSi on the right and (b) with NdFeB on the left and FeCo on the right (The magnetic field lines are estimated as the influence of the presence of the as-printed specimens within the external field)

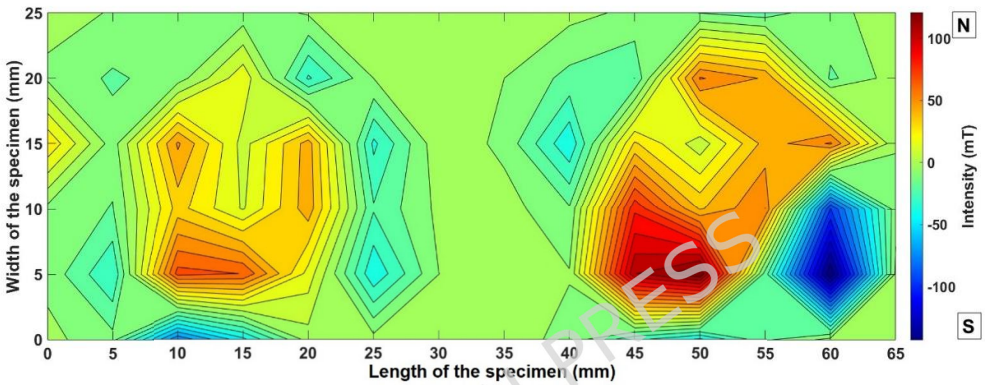

(a) NdFeB on the left and FeSi on the right

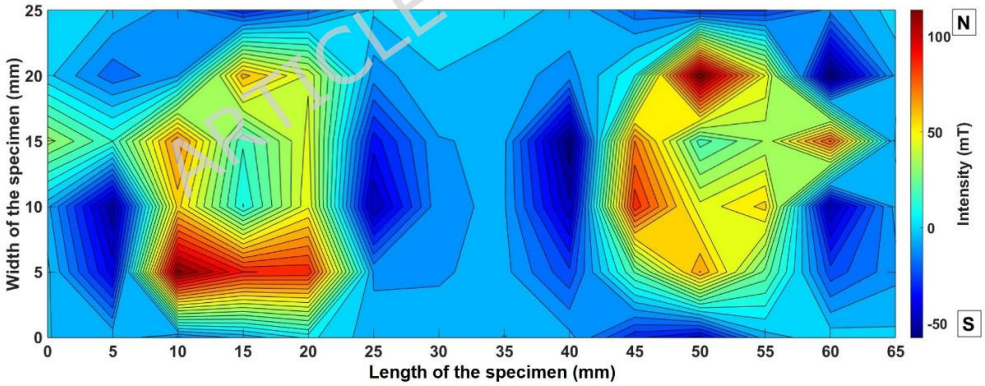

(b) NdFeB on the left and FeCo on the right

Fig. 10 Iso-magnetic field lines plotted on the top surfaces of laser sintered multiple magnetic material samples in nylon matrix after magnetising in a 1.9T north upward field and under a north upward external magnetic field of 230 mT acting under the two islands (a) with NdFeB on the left and FeSi on the right and (b) with NdFeB on the left and FeCo on the right (The magnetic field lines are

estimated as the influence of the presence of the printed specimen within the external field)

The magnetic contour patterns obtained on the same samples after magnetising with a 1.9 T north upward field and then measured under the influence of a 230 mT applied field are in similar lines, as shown in Fig 10. However, the magnetisation along the magnetic easy axis (north upward) resulted in higher magnetic field strengths in both cases, with a 100 mT north and around 50 mT south polar responses. The higher -150 mT island seen as a stray dispersion in a small area in Fig 10 (a) is mostly due to an accidental excessive deposition of FeSi powder, which has proved to be more difficult to control while laser sintering under external magnetic fields.

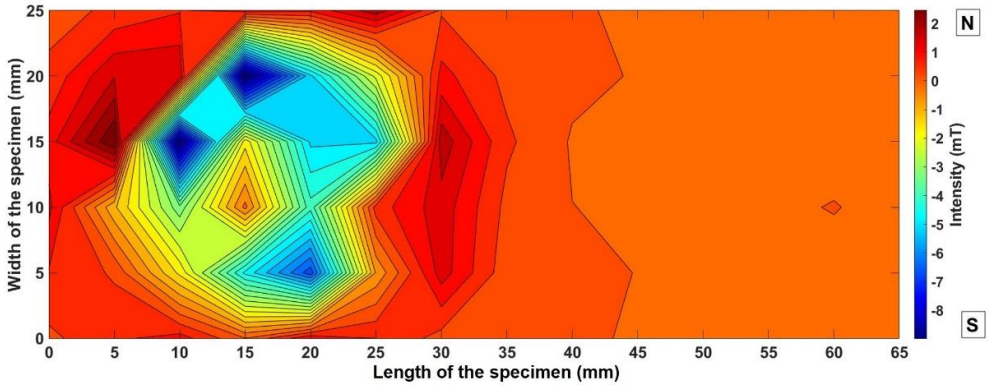

(a) NdFeB on the left and FeSi on the right

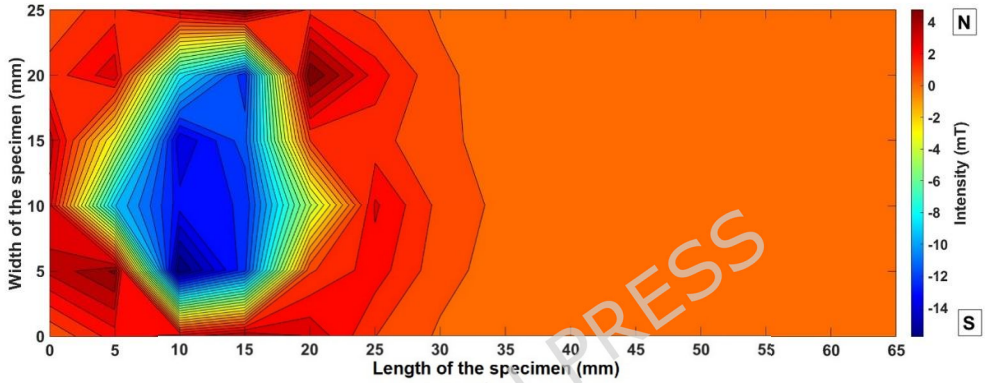

(b) NdFeB on the left and FeCo on the right

Fig. 11 Iso-magnetic field lines plotted on the top surfaces of laser sintered multiple magnetic material samples in nylon matrix after magnetising in a 1.9T north downward field (a) with NdFeB on the left and FeSi on the right and (b) with NdFeB on the left and FeCo on the right

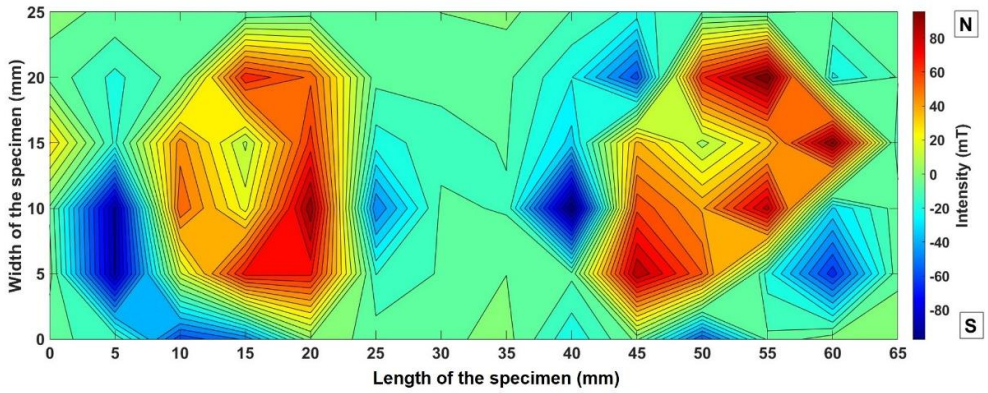

(a) NdFeB on the left and FeSi on the right

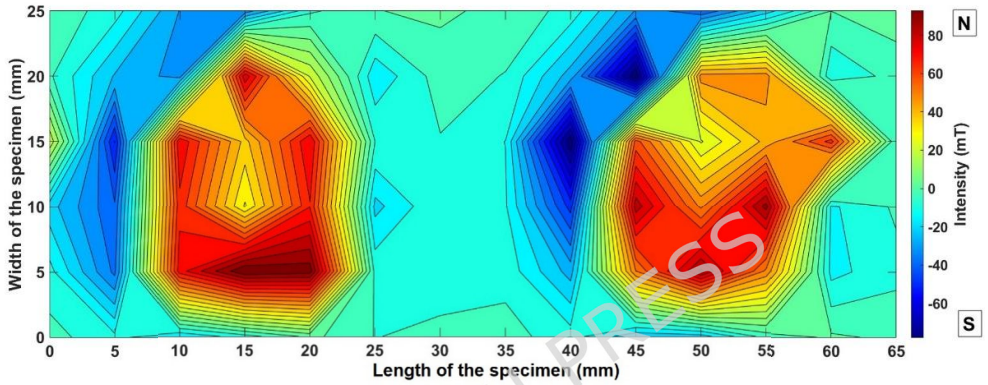

(b) NdFeB on the left and FeCo on the right

Fig. 12 Iso-magnetic field lines plotted on the top surfaces of laser sintered multiple magnetic material samples in nylon matrix after magnetising in a 1.9 T north downward magnetic field and under the influence of a north upward external magnetic field of 230 mT acting under the two islands (a) with NdFeB on the left and FeSi on the right and (b) with NdFeB on the left and FeCo on the right (The magnetic field lines are estimated as the influence of the presence of the as-printed specimens within the external field)

After magnetising in a North downward reverse field at 1.9 T, the two samples responded to the remnant magnetic field measurements as depicted in Fig 11 (a) and (b) with the NdFeB/FeSi and the NdFeB/FeCo cases respectively. The reverse magnetic field has caused a dramatic flip

in the north and south pole orientations around the NdFeB regions. Comparing the results in Figs 8(a) and (b) with those in Fig 11 (a) and (b), what is a north central and south surrounding pattern has changed to a south central and north surrounding field pattern in the latter case due to the magnetisation under the reverse field. Also, it is pertinent to point out that the maximum north-ward field intensity reduced from 6 mT and 14 mT to 2 mT and 4 mT in the corresponding results in Fig 8 and Fig 11 respectively, indicating the directional magnetic nature and the upward orientation of the magnetic easy axes as imposed during the laser sintering stages with the application of the external magnetic field. The rest of the areas remain with almost negligible magnetic remanence due to the soft nature of the FeSi and FeCo regions.

Finally, the magnetic contours obtained based on the two samples after magnetising under a north downward reverse field of 1.9T and measured under an external upward field of 230 mT are presented in Fig 12. It is interesting to make some observations comparing the magnetic field results of Fig 10 and Fig 12. The conditions are all the same, but the only difference is that the upward magnetising field in Fig 10 is reversed to obtain the results in Fig 12. The patterned magnetic pole configurations [18] are very similar in both cases. However, there is about a 20% reduction in the field strength at the north pole regions in both the samples in Fig 12 due to the reversal of the magnetic field. This is indicative of the north upward easy axis as imposed by the direction of the external magnetic field

applied during sintering. Further, the widely spread south pole domains are reduced to a couple of narrow zones on either side of the sample in Fig 12 (b). It appears that dipolar coupled systems are formed in both Fig 10(a) and Fig 12 (b) leading to the demagnetisation of the material in the central regions due to opposing magnetic domain interactions [3].

Quantitative consolidation

Following these results and discussion, a quantitative consolidation of the inferences is attempted by compiling the key results and observations as listed in Table 1.

Table 1 Compilation of quantitative observations

Magnetic material used in the two islands and the directions of external field	Maximum field intensity in as-printed state	Maximum field intensity after magnetising under a	Other observations
Both NdFeB , and 230 mT north upward	2.0 mT N and 1.5 mT S (Fig 5 (a))	**1.5 T North upward field** 2mT N and 0.5 mT S (Fig 6(a))	Widely dispersed multi-polar dispersions
Both NdFeB , 230 mT South upward on the left and North upward on the right	1.5 mT S (left) and 0.5 mT N (right) (Fig 5 (b))	**1.5 T North upward field** 2 mT N and 3.5 mT S (Fig 6(b))	North-South dipolar on the left and clear north pole on the right
NdFeB on the left and FeSi on the right , 230 mT North upward field at both ends	2mT N and 4.5 mT S Left 0 mT remanence Right (Fig 7 (a))	**1.9 T North upward field** 6 mT N and 3 mT S Left 0 mT remanence Right (Fig 8(a))	Dispersed south pole around the central north on the left
NdFeB on the left and FeCo on the right , 230 mT North upward field at both ends	1.5 mT N and 2 mT S 0 mT remanence Right (Fig 7 (b))	**1.9 T North upward field** 14 mT N and 6 mT S Left 0 mT remanence Right (Fig 8(b))	Dispersed south pole around the central north on the left
NdFeB on the left and FeSi on the right , 230 mT North upward field at both ends	**within the external field** 80 mT N and 80 mT S (Fig 9 (a))	**1.9 T North upward field within the external field** 100 mT N and 100 mT S (Fig 10 (a))	Scattered North islands and scattered South all around
NdFeB on the left and FeCo on the right , 230 mT North upward field at both ends	**within the external field** 100 mT N and 50 mT S (Fig 9 (b))	**1.9 T North upward field within the external field** 100 mT N and 50 mT S (Fig 10 (b))	Scattered North islands and Scattered South all around
NdFeB on the left and FeSi on the right , 230 mT North upward field at both ends	-	**1.9 T North downward field** 2 mT N and 8 mT S Left 0 mT remanence Right (Fig 11(a))	The North and South regions flipped
NdFeB on the left and FeCo on the right , 230 mT North upward field at both ends	-	**1.9 T North downward field** 4 mT N and 14 mT S Left 0 mT remanence Right (Fig 11(b))	The North and South regions flipped

NdFeB on the left and FeSi on the right , 230 mT North upward field at both ends	-	**1.9 T North downward field within the external field** 80 mT N and 80 mT S (Fig 12 (a))	North islands and South surrounding North pole intensity reduced. Slight reduction in North intensity
NdFeB on the left and FeCo on the right , 230 mT North upward field at both ends	-	**1.9 T North downward field within the external field** 80 mT N and 60 mT S (Fig 12 (b))	North Islands and South surrounding. Slight reduction in North intensity

The following are the most significant observations made and the inferences drawn from these results:

- In the as printed condition, the NdFeB islands created in nylon matrix under a North upward magnetic field result in a 1.5 mT South pole islands surrounded by a 1.5 mT dispersed North polar regions.
- With the South-upward left and North upward right magnetic field, the same combination as above results in a focussed 1.5 mT South pole on the left and a 0.5 mT North pole on the right in the as printed state.
- After magnetising under a 1.5 T North upward field, the above samples achieve a 2 mT North polar regions with varying degrees of South pole intensities, and a patterned polar dispersion in the first case and a clear dipolar dispersion in the second case.
- In the as printed condition, the two samples with NdFeB/FeSi and NdFeB/FeCo islands achieved 2mT N/4.5mT S and 1.5 mT N/2 mT S flux values respectively at the hard magnetic pole while the soft magnetic regions show zero magnetic remanence.
- Once magnetised under a 1.9T external field, the same samples as above reach 6mT N/3mT S and 14 mT N/6 mT S flux values

respectively at the hard magnetic pole while the soft magnetic regions show zero magnetic remanence.

- Both NdFeB/FeSi and NdFeB/FeCo samples show around 80 to 100 mT N and 50 to 100 mT S differential polarities under the influence of an external magnetic field with only minor variations in responses from the as-printed to the post-printing magnetisation under a 1.9 T external field.
- Flipping the external magnetic field shows the expected increase in the south polar regions, while there is still significant North upward polar tendency remains indicating the remanent magnetic easy direction imposed by the external field during laser consolidation.

Conclusion

The hypothesis that the point-wise material consolidation mechanics typical of additive technologies can be used to achieve controlled dispersion of multiple magnetic fields with pre-set directions for the magnetic easy axes is tested in this research. For this, controlled dispersion of different magnetic material particles into polymer matrices and layer wise consolidation by selective laser sintering are implemented to make bonded magnets with and without the use of external magnetic fields. Hard magnetic NdFeB and soft magnetic FeSi and FeCo materials in powder form are used as the magnetic material options and polyamide as the matrix material. Dipolar bonded magnetic substrates are created with NdFeB at both poles and NdFeB/FeSi and NdFeB/FeCo at either ends as combinations. The direction of application of the external magnetic fields around the two

magnetic material regions are also varied to ascertain the possible control over the directionality of the magnetic easy axes of the consolidated polar regions.

Microstructural observations and Bitter pattern images confirmed the influences of the external magnetic fields in controlling the consolidation mechanics as well as the magnetic domain mapping responses. Iso-magnetic field contours plotted from Gauss meter probe measurements elucidated patterned magnetic pole configurations that can be tailored by controlled dispersion of different magnetic materials in the polymer matrix. Dynamic variations in the patterns of magnetic pole configurations are noted from the as printed to the magnetised states of printed specimens with the external fields aligned and opposing the orientations of the magnetic easy axes as imposed during laser sintering. The resulting magnetic polar dispersions follow specific patterns in accordance with the magnetic materials dispersed, the directions of the external fields used during sintering and the direction of post-printing magnetisation. It is ascertained that controlled magnetic heterogeneity can be achieved using suitable combinations of all these parameters.

Looking ahead, the ability to print magnets with spatially programmed hard or soft regions and easy-axis orientations could enable compact electromagnetic devices with integrated field shaping such as graded actuators, motors, and maglev components where electro-mechanical coupling is critical [20]. Moreover, heterogeneous magnets could serve as building blocks for functional and reconfigurable systems, including

magnetically switchable or shape-morphing devices and magnetically controlled millirobots operating across air–water interfaces [21].

Funding

The authors wish to acknowledge the support received by the Marsden Fund Grant No. MFP AUT1901 from the Royal Society of New Zealand Te Apārangi in carrying out the research reported in this paper

Data Availability

The datasets used and/or analysed during the current study available from the corresponding author on reasonable request.

References

1 Huber, C., et al. "3D print of polymer bonded rare-earth magnets, and 3D magnetic field scanning with an end-user 3D printer." *Applied Physics Letters* 109.16 (2016).

2 Li, Ling, et al. "Fabrication of highly dense isotropic Nd-Fe-B nylon bonded magnets via extrusion-based additive manufacturing." *Additive Manufacturing* 21 (2018): 495-500.

3 Domingo-Roca, R., J. C. Jackson, and J. F. C. Windmill. "3D-printing polymer-based permanent magnets." *Materials & Design* 153 (2018): 120-128.

4 Huber, Christian, et al. "Additive manufactured polymer-bonded isotropic NdFeB magnets by stereolithography and their comparison to fused filament fabricated and selective laser sintered magnets." *Materials* 13.8 (2020): 1916.

5 Wendhausen, P. P., et al. "Additive manufacturing of bonded NdFeB, process parameters evaluation on magnetic properties." *2017 IEEE International Magnetics Conference (INTERMAG)*. IEEE, 2017.

6 Mapley, Martin, et al. "Selective laser sintering of bonded magnets from flake and spherical powders." *Scripta Materialia* 172 (2019): 154-158.

7 Mapley, Martin, et al. "Influence of powder loading fraction on properties of bonded permanent magnets prepared by selective laser sintering." *3D Printing and Additive Manufacturing* 8.3 (2021): 168-175.

8 Zhang, Fenghua, et al. "Magnetic programming of 4D printed shape memory composite structures." (2019): 105571.

9 Wu, Hongzhi, et al. "Selective laser sintering-based 4D printing of magnetism-responsive grippers." *ACS applied materials & interfaces* 13.11 (2020): 12679-12688.

10 Zhai, Haorui, et al. "4D printing of Nd-Fe-B composites with both shape memory and permanent magnet excitation deformation." *Composites Part A: Applied Science and Manufacturing* (2024): 108443.

11 Henderson, Lauren, et al. "Altering magnetic properties of iron filament PLA using magnetic field assisted additive manufacturing

(MFAAM)." *Journal of Magnetism and Magnetic Materials* 538 (2021): 168320.

12 Sarkar, Abhishek, M. Parans Paranthaman, and Ikenna C. Nlebedim. "In-situ magnetic alignment model for additive manufacturing of anisotropic bonded magnets." *Additive Manufacturing* 46 (2021): 102096.

13 Afshari, Pantea, et al. "Mechanical strain tailoring via magnetic field assisted 3D printing of iron particles embedded polymer nanocomposites." *Macromolecular Materials and Engineering* 308.11 (2023): 2300194.

14 Mapley, Martin Christopher, et al. "Selective laser sintering of bonded anisotropic permanent magnets using an in situ alignment fixture." *Rapid Prototyping Journal* 27.4 (2021): 735-740.

15 Kokkinis, Dimitri, Manuel Schaffner, and André R. Studart. "Multimaterial magnetically assisted 3D printing of composite materials." *Nature communications* 6.1 (2015): 8643.

16 Koyalamudi, Kiran Babu, Ruoyu Yang, and Rahul Rai. "Additive Manufacturing of Conductive Polymer Nanocomposites Under the Influence of External Magnetic Field." *International Design Engineering Technical Conferences and Computers and Information in Engineering Conference*. Vol. 50077. American Society of Mechanical Engineers, 2016.

17 Lu, Lu, Ping Guo, and Yayue Pan. "Magnetic-field-assisted projection stereolithography for three-dimensional printing of smart

structures." *Journal of Manufacturing Science and Engineering* 139.7 (2017): 071008.

18 Kim, Yoonho, et al. "Printing ferromagnetic domains for untethered fast-transforming soft materials." *Nature* 558.7709 (2018): 274-279.

19 Nagarajan, Balakrishnan, et al. "Characterization of magnetic particle alignment in photosensitive polymer resin: A preliminary study for additive manufacturing processes." *Additive Manufacturing* 22 (2018): 528-536.

20 Zheng, J., et al. "Potential and Electro-Mechanical Coupling Analysis of a Novel HTS Maglev System Employing Double-Sided Homopolar Linear Synchronous Motor." IEEE Transactions on Intelligent Transportation Systems 25(10) (2024): 13573-13583. doi: 10.1109/TITS.2024.3398148.

21 Zhang, Z., et al. "Magnetically Switchable Adhesive Millirobots for Universal Manipulation in both Air and Water." Advanced Materials 37(26) (2025): 2420045. doi: 10.1002/adma.202420045.

22 Zhou, P., Qi, H., Zhu, Z., Qin, H., Li, H., Chu, C., & Yan, M. (2018). Development of SiC/PVB composite powders for selective laser sintering additive manufacturing of SiC. Materials, 11(10), 2012.